

Simultaneous observations of optical and electrical signals in altitude-triggered negative lightning flashes

Mingli Chen,¹ Teiji Watanabe,² Nobuyuki Takagi,² Yaping Du,¹ Daohong Wang,² and Xinsheng Liu³

Received 20 June 2002; revised 26 November 2002; accepted 30 January 2003; published 18 April 2003.

[1] This paper presents an analysis of the experimental data on five negative lightning flashes initiated using the altitude-triggering technique in China. The data include highly time-resolved optical images and electric fields measured 60 m and 1300 m from the lightning channel. The triggering technique involves the launching upward of a small rocket trailing a wire electrically floating. The data show that these 5 flashes have a similar chronological sequence of events, including a bidirectional leader system followed by a mini-return stroke and a bidirectional discharge process. The bidirectional leader system consists of an upward positive leader initiated from the top of the wire and a downward negative stepped leader from the bottom, with the onset of the former prior to the latter by 3 to 8.3 ms. The downward negative stepped leader, having a step interval of 12–30 μ s, appears to pause and resume several times while the upward positive leader extends forward continuously. With the downward negative stepped leader close to ground, a mini-return stroke occurs between the ground and the bottom of the wire. The mini-return stroke propagates upward with a speed of $1\text{--}2 \times 10^8$ m/s and emits intense light signals similar to a normal return stroke below the bottom of the wire. It becomes invisible after entering the bottom of the wire and appears again as a bright upward discharge from the top of the wire several microseconds later. This upper bright discharge ceases after propagating forward several hundred meters at a speed of $1.5\text{--}5.4 \times 10^7$ m/s. The cessation of the upper bright discharge is obviously associated with the disintegration of the wire at that moment. Right after the cessation of the upper bright discharge, a bidirectional discharge process starts from the bottom of the wire with its positively charged part having an upward speed of $3\text{--}10 \times 10^5$ m/s and its negatively charged part a downward speed of $2\text{--}2.6 \times 10^5$ m/s. Reflection of current waves at the bottom of the wire due to the explosion of the wire at that moment may be a major reason for the occurrence of this lower bidirectional discharge. **INDEX TERMS:** 3304 Meteorology and Atmospheric Dynamics: Atmospheric electricity; 3324 Meteorology and Atmospheric Dynamics: Lightning;

KEYWORDS: altitude-triggered lightning, bidirectional leader, mini-return stroke

Citation: Chen, M., T. Watanabe, N. Takagi, Y. Du, D. Wang, and X. Liu, Simultaneous observations of optical and electrical signals in altitude-triggered negative lightning flashes, *J. Geophys. Res.*, 108(D8), 4240, doi:10.1029/2002JD002676, 2003.

1. Introduction

[2] The “altitude-triggered lightning technique” refers to triggering a lightning flash by launching upward a small rocket trailing an electrically floating wire, with the bottom of the wire being typically some hundreds of meters above the ground (Figure 1). Lightning triggered by using this technique usually has a predictable ground strike point within a few hundred meters of the launcher, which is a

great advantage for making measurements of close lightning. In addition to this, an altitude-triggered lightning flash always involves a bidirectional leader system initiated from the extremities of the floating wire followed by an “abnormal” first return stroke called “mini-return stroke” [Laroche *et al.*, 1991; Lalande *et al.*, 1998; Rakov *et al.*, 1998]. The bidirectional leader system is composed of an upward positive leader from the top of the wire and a downward negative stepped leader from the bottom of the wire under negatively charged thunderclouds. These properties make the altitude-triggered lightning technique a valuable tool for the study of leader development and the attachment process, which are two extremely important aspects for the protection of structures against lightning, and can only be well understood by making measurements of close lightning.

[3] From the electrical field measurements made simultaneously with the electric currents and streak photographs for two altitude-triggered negative lightning flashes, Laroche *et*

¹Department of Building Services Engineering, Hong Kong Polytechnic University, Kowloon, Hong Kong.

²Department of Electrical and Electronic Engineering, Gifu University, Gifu, Japan.

³Cold and Arid Regions and Environmental Engineering Institute, Chinese Academy of Sciences, Lanzhou, China.

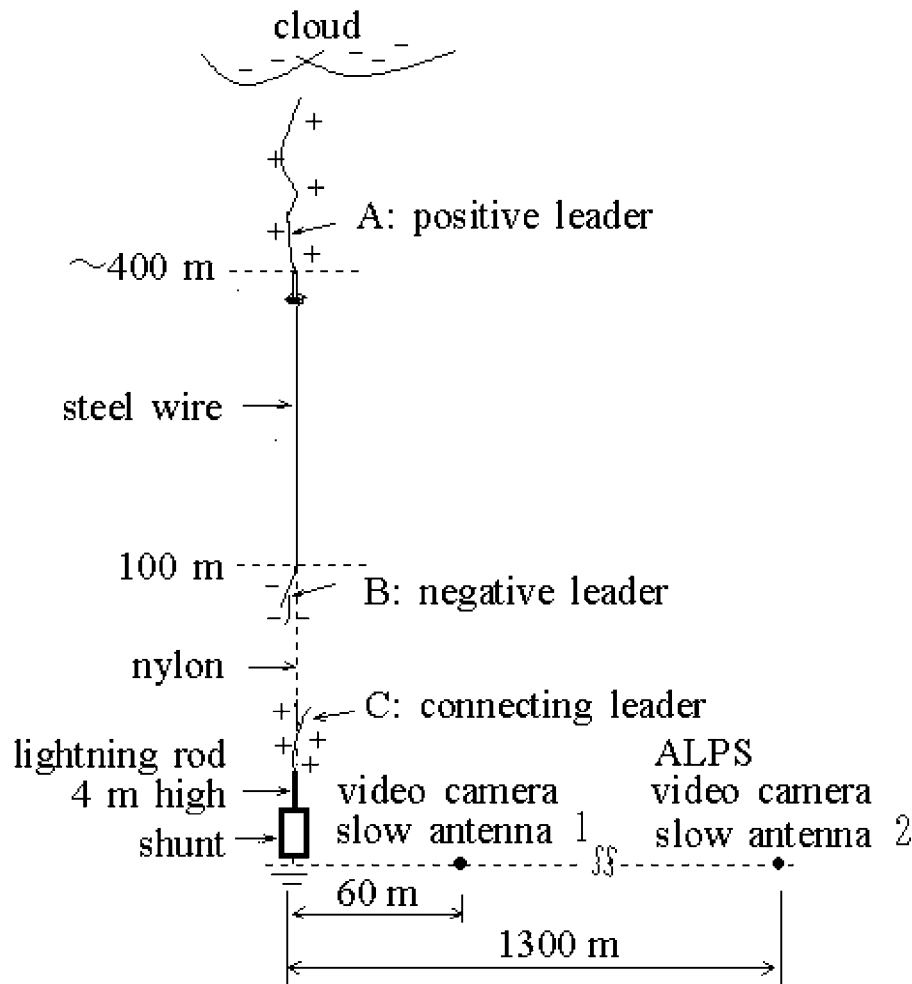


Figure 1. Illustration of the altitude-triggered lightning technique used in the experiment and the setup of the observation sites.

al. [1991] and *Lalande et al.* [1998] studied in detail the properties of inception and propagation of the bidirectional leader systems involved. They found that the onset of the upward positive leader is prior to that of the downward negative leader by about 3 ms and 6 ms for the two flashes, respectively. However, they did not address significantly the relevant mini-return strokes, probably due to the limitation of time resolution of the streak cameras they used. The only description of the properties of the mini-return stroke of an altitude-triggered lightning flash, as inferred from the electric and magnetic field measurements, can be found in the literature of *Rakov et al.* [1998].

[4] This study investigates both the bidirectional leader system and the following mini-return stroke involved in an altitude-triggered lightning flash, by simultaneously making measurements of highly time-resolved optical images and electric fields at close distances.

2. Instrumentation and Data

[5] The data analyzed in this study were acquired in a rocket-triggered lightning experiment conducted in the

suburbs of Guangzhou, southern China, during the summer of 1998. The altitude-triggered lightning technique used in this experiment was similar to that employed in the rocket-triggered lightning experiment at Camp Blanding, Florida [*Rakov et al.*, 1998]. The only differences involve the bottom heights of the floating wire and the length of the grounded intercepting wire. As shown in Figure 1, after its launch the rocket first spooled out about 100 m of an electrically insulated nylon cable from the bobbin attached to the rocket tail, and then a steel wire was unreeled. The nylon cable was fixed to a 4-m-high lightning rod grounded via a current measuring system. The wire was a kind of commercial stainless wire used for piano strings, with a diameter of 0.2 mm.

[6] Measurements were carried out at two sites. Site 1 was located at a distance of about 60 m from the launcher and Site 2 about 1300 m from the launcher. Electric fields were measured at both sites by using a flat-plate slow antenna system. The signals of the antenna were integrated and recorded on a computer with a sampling rate of 12.5 MHz, a digital resolution of 12 bits, and a recording length of 2 mega words per event. The resultant band-width of the

slow antenna system was 4 Hz–1.5 MHz. For recording the luminous progression of lightning channels, a high-speed digital imaging system named Automatic Lightning Progressing Feature Observation System (ALPS) was deployed at Site 2. The ALPS includes a conventional camera lens, a pin photodiode array module, amplifiers, a multichannel digitizer, and a personal computer system. The photodiode array module consists of 256 pin photodiodes ($16 \text{ rows} \times 16 \text{ columns}$, pin size is $1.3 \times 1.3 \text{ mm}^2$) mounted in the focal plane behind the lens, with the separation between the centers of individual photodiodes being 1.5 mm. Signals from the photodiode array are amplified, digitized, and then recorded on the computer system. The whole system of the ALPS can operate at a time resolution of 100 ns to 50 ms with either an internal or external trigger mode and can record up to 16,000 frames for each event with up to 100% pretrigger frames. More information on the ALPS can be found in the papers of Wang *et al.* [1999] and Chen *et al.* [1999a]. The time resolution used in this experiment was 100 ns, and the resultant total recording time per event was 1.6 ms with a pretrigger time of 1120 μs . The lens focal distance used in this study was 35 mm. This value in conjunction with the size of the pin photodiode yields a spatial resolution of about 55 m for the lightning flashes triggered in this experiment. During the observation, the ALPS worked at internal trigger mode and its output of the trigger signal was used to trigger the slow antenna system at Site 2 to synchronize the time of these two measurements. In addition to the above measurements, two common digital video cameras (60 frames per second) were also deployed at the two sites, with the camera at Site 1 being focused on the bottom hundred meters of the lightning channel, and that at Site 2 the whole lightning channel.

[7] There are a total of five triggered-lightning flashes, numbered CHN9801, CHN9802, CHN9803, CHN9804 and CHN9805, for which simultaneous records including the ALPS images, the two-station electric fields and the video camera images have been obtained during the experiment. All five of these flashes were triggered at a time interval of 3 to 5 min during the period from 1641 to 1701 LT (local time) in a local convection storm on August 22, when the electric field intensity at ground level was about -6 to -10 kV/m (negatively charged clouds produce a negative electric field at ground level). The electric field records indicate that all five of these flashes are typical of negative flashes (lowering negative charges to the ground) with a characteristic initial leader developing stage followed by a mini-return stroke. Since these five flashes behave in a similar way, only the flash CHN9805 is examined in detail in the following text to substantiate our observation results.

3. Results and Analysis

[8] The video records allow us to examine the overall spatial characteristics of a flash, including the ground striking point, the triggering height, the branches, and the channel declination. Figure 2a is a picture of flash CHN9805 selected from the video records at Site 1, and Figure 2b a picture at Site 2. As shown in Figure 2a, this flash strikes the ground about 60 m to the right of the

launcher with a decline angle of about 30 degrees. Apparently, the bottom 100 m of the discharge channel is not associated with the trace of the nylon cable fixed to a lightning rod near the launcher. Figure 2b shows the whole channel of the flash. The straight bright line in the figure is associated with the melting of the triggered wire, and the low luminous part is associated with the lightning channel in the air. As seen in the figure, the triggering height is about 350 m, and the channel branches into two at the height of about 600 m above ground. On the video records, the appearance of the branch in the left is prior to the branch in the right by one frame (16 ms).

[9] Figures 3a and 3b are the electric field records of flash CHN9805 at Site 1 and Site 2 respectively, and Figures 4a and 4b are the ALPS records of the same flash at Site 2. In the following, the analysis of the events before the mini-return stroke is mainly based on the electric field records, and the analysis around and after the mini-return stroke is mainly based on the ALPS records. For analytical convenience, the time 0 at both sites is set to the peak time of the electric waveform of the mini-return stroke. In case the peak is flat due to saturation, the central point of the flat part of the mini-return stroke waveform is set to time 0, with the error being less than 1 μs . The resultant recording time for the electric fields is from -50 ms to 110 ms and that for the ALPS from -1.12 ms to 0.48 ms .

3.1. Bidirectional Leader System Before the Mini-Return Stroke

[10] In the electric fields at Site 1 (Figure 3a), there are two small isolated field steps appearing at the times -35 ms and -22 ms , respectively. The amplitudes of these two field steps are about -20 V/m and -40 V/m , and their 10–90% down-edge-times are about 0.8 μs and 1.2 μs , respectively. No corresponding radiation pulses are identified in the electric fields at Site 2 (Figure 3b). As the floating wire is ascending under negatively charged thunderclouds, the quasi-static electric field of the thunderclouds tends to induce a positive charge concentrating at the upper part of the wire and a negative charge at the lower part of the wire. If we suppose that an electric field step is caused by the sudden emerging of two opposite point charges at the extremities of the wire, and if the heights of the extremities of the wire at the moment are available, the magnitude of the point charge can be estimated through the application of a simple electrostatic formula [Lalande *et al.*, 1998]. Further, if the down-edge-time of a field step is available, a transit current that must flow in the wire to transfer the charge within the down-edge-time can be estimated by simply dividing the amount of the charge over the down-edge-time. The field step at -35 ms is consistent with a charge of $-20.2 \mu\text{C}$ at the bottom of the wire (100 m above ground) and a charge of $+20.2 \mu\text{C}$ at the top of the wire (350 m above ground at the moment), and a transit current of about 20 A. The field step at -22 ms is consistent with a charge of $-40.4 \mu\text{C}$ at the bottom of the wire and $+40.4 \mu\text{C}$ at the top, and a transit current of about 27 A. As will be discussed in section 4.1, such an electric field step may be attributed to an attempt of the inception of an upward positive leader from the top of the wire.

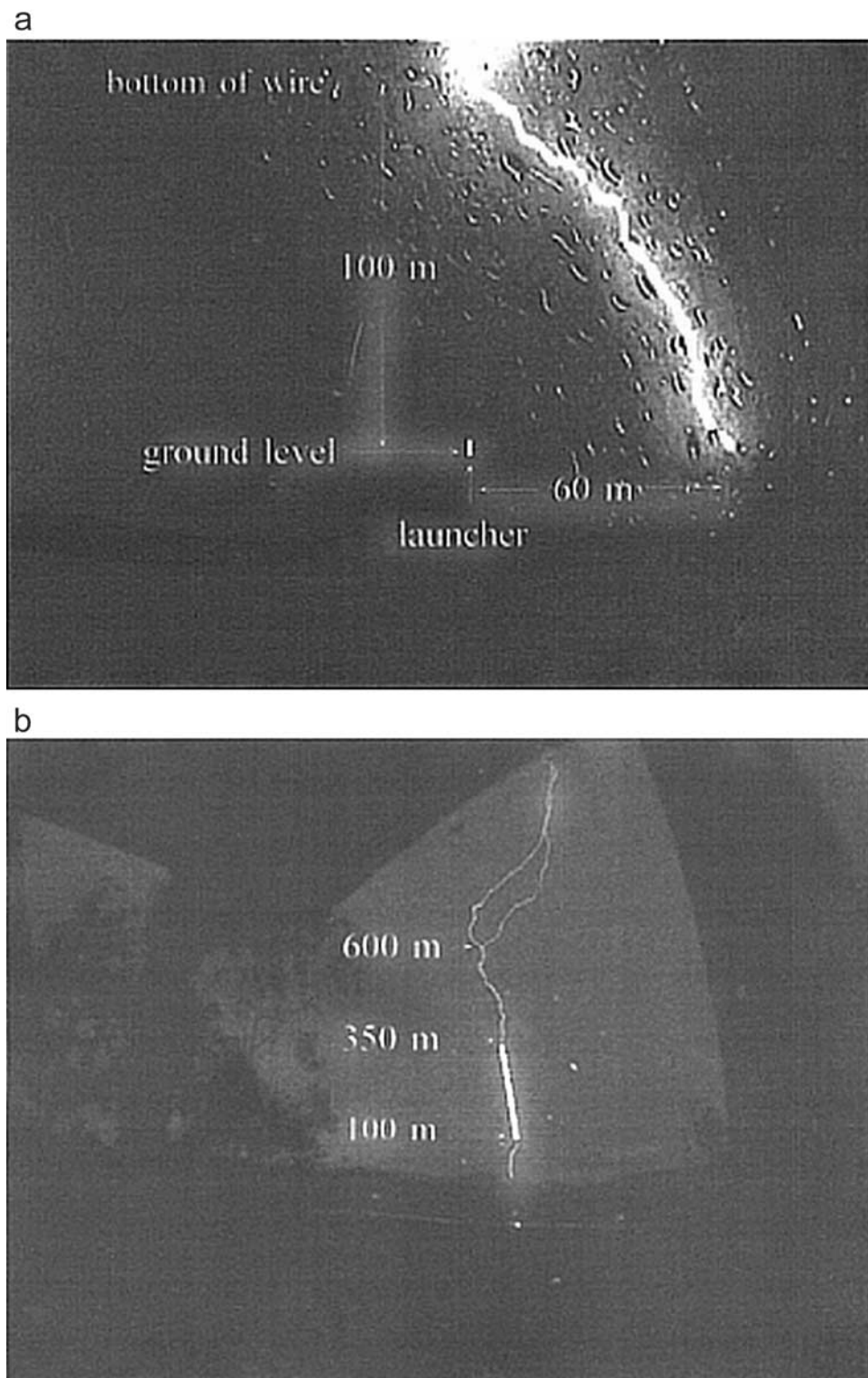


Figure 2. (a) A picture selected from the video records at Site 1 (60 m from the launcher) showing the bottom 100 m of the channel, and (b) a picture from the video records at Site 2 (1300 m from the launcher) showing the whole channel, for flash CHN9805 at 1700:48.66 (local time) on August 22, 1998, China.

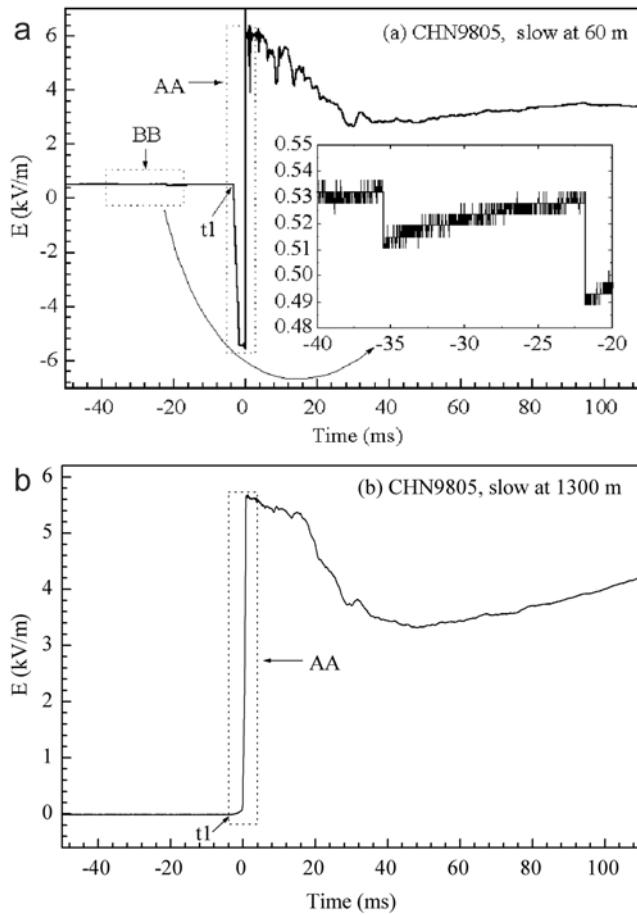


Figure 3. Overall time waveforms of the electric fields recorded by using the flat-plate slow antenna systems (total recording time: -50 ms to 110 ms) at (a) Site 1 and (b) Site 2 for flash CHN9805. The time 0 for both sites is associated with the peak of the electric field pulse produced by the mini-return stroke.

[11] About 18.6 ms after the last isolated field step, from time t_1 ($t_1 = -3.4$ ms), the electric field at Site 1 (Figure 5a; the flat part after time -1.7 ms is due to the saturation of the slow antenna system) begins to decrease first step-wisely and then continuously. There are a total of 11 field steps around the time t_1 , with the step interval being about 20 – 30 μ s. The field steps have a mean amplitude of -64 V/m and a mean 10 – 90% down-edge-time of 0.64 μ s, which are consistent with a charge of ± 65 μ C at the two ends of the floating wire and a transit current of about 100 A. They may be associated with some step-wise discharge processes of either an upward positive leader from the top of the wire or a downward negative leader from the bottom of the wire. The continuously changing part has a mean slope of -3530 kV/m/s during the time t_1 to -2.0 ms. Assuming this field slope is associated with a continuous current that transfers charges between the two ends of the wire, the magnitude of the current can be estimated in the same way used for the field steps. The decreasing slope of -3530 kV/m/s, dominated by the negative charge deposited at the lower part of the wire, is consistent with a continuous current of about 3.6 A in the wire. It should be associated with a continuous

propagation of an upward positive leader developing from the top of the triggered wire.

[12] Meanwhile, from t_1 , the electric field at Site 2 (Figure 5b) begins to increase with several bipolar pulse trains superimposed on a continuously rising slope. The pulse train around t_1 has a pulse number of 11 and an inter-pulse interval of 20 – 30 μ s, similar values to those of the field steps around t_1 at Site 1 (Figure 5a). The mean positive peak of this pulse train is about 12 V/m and its mean pulse p-p width (the time difference between the positive peak and negative peak for a bipolar pulse) about 0.96 μ s. Apparently, these bipolar field pulses are radiated by the pulse currents injected inside the wire when the upward positive leader starts its development. The increasing slope during t_1 to -2.0 ms, about 8.5 kV/m/s in mean, is consistent with a continuous current of 4.8 A, a similar value to that derived from the electric field at Site 1 for the same time period.

[13] During t_1 to t_2 ($t_2 = -348$ μ s), the electric field step/pulse trains appear and disappear several times at both sites (e.g., the pulse trains appearing at time -3.4 ms, -1.6 ms, -1.0 ms, and -348 μ s in Figures 5a and 5b), while the fields at Site 2 (Figure 5b) increase continuously. This indicates that the downward negative stepped leader pauses and resumes several times while the upward positive leader extends forward continuously. The electric field slope at Site 2 increases from about 8.5 kV/m/s before -1.6 ms to 43.3 kV/m/s after that time. The later is consistent with a continuous current of about 25 A. This field slope increase indicates that the upward positive leader begins to speed up after the resumption of the downward negative leader at the time -1.6 ms. The light records of ALPS show that the bottom end of the wire begins to light at least from the time -1.1 ms with two light pulse trains appearing at the times -1.0 ms and t_2 , respectively (Figure 6). Apparently, the continuous luminosity at the bottom end of the wire is associated with the local negative corona discharge driven by the upward positive leader. The light pulse trains are certainly associated with the successive steps of the downward negative leader.

[14] The downward negative stepped leader seems to enter its stable propagation regime from time t_2 , as both the light pulses (Figure 6) and the electric field steps/pulses (Figures 7a and 7b) appear uninterruptedly from that moment. Figures 8a, 8b and 8c are the expansions of portion “a” in Figure 6, portion “A-a” in Figure 7a, and portion “A-a” in Figure 7b, respectively. Figures 9a, 9b and 9c are the expansions of portion “b” in Figure 6, portion “A-b” in Figure 7a and portion “A-b” in Figure 7b, respectively. Comparing the Figures 8 and 9, both the field and light pulses of the first 12 steps during -340 μ s to -180 μ s (numbered 1–12 in Figure 8) have distinctly different shapes from those of the following 15 steps during -180 μ s to -10 μ s (numbered 13–27 in Figure 9). Each of the first 12 steps produces a distinguishable light pulse (Figure 8a), a double-peak-humpy field change at Site 1 (Figure 8b), and a bipolar electric field pulse with a p-p width of about 2 μ s at Site 2 (Figure 8c). By comparison, each of the following 15 steps produces an indistinguishable light pulse (Figure 9a), a single-peak-humpy field change at Site 1 (Figure 9b), and a unipolar field pulse with a half-peak width of 0.4 μ s at Site 2 (Figure 9c). The average time

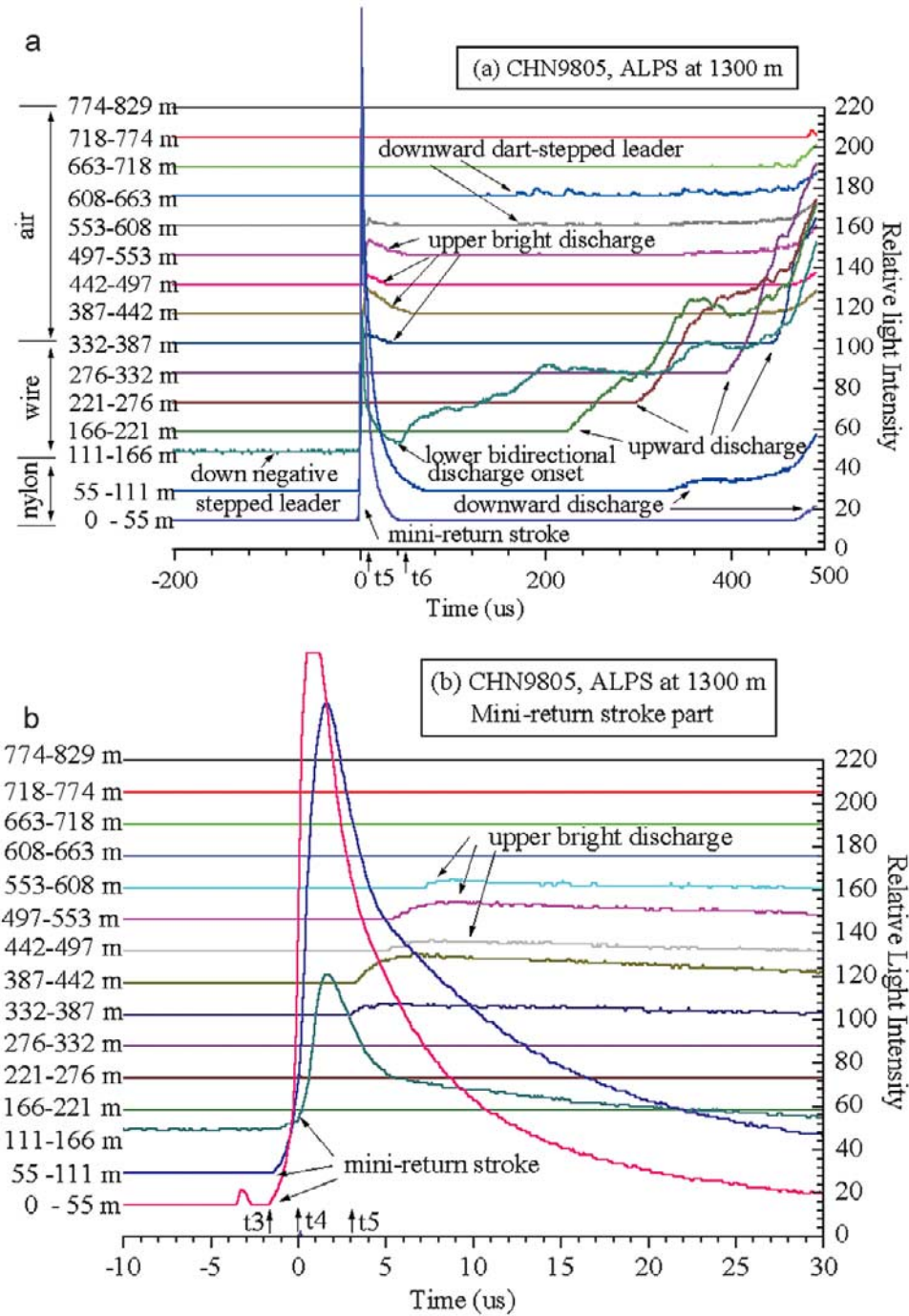


Figure 4. Waveforms of the light signals versus heights and times recorded by using the ALPS (total recording time -1.1 ms to 0.5 ms) at Site 2 for flash CHN9805. Time is synchronized with the electric field records at Site 2. (a) The records for the period from time -200 μ s to 500 μ s, and (b) those for the mini-return stroke period from time -10 μ s to -30 μ s. It should be noted that before the mini-return stroke only the segment 111–166 m, the bottom end of the floating wire, is optically detectable to the ALPS.

interval for the first 12 steps is about 15 μ s, and that for the following 15 steps about 12 μ s. The transit current involved in each step in this stage, by comparing the amplitude of the field pulses around t_2 in Figures 8c and 9c (positive peak: 16 – 64 V/m) with that around t_1 in Figure 5b (positive peak:

12 V/m; transit current: 100 A), is estimated to be between 130 A and 530 A. Meanwhile, the field slope at Site 2 increases from 325 kV/m/s during -340 μ s to -180 μ s (Figure 8c) to 635 kV/m/s during -180 μ s to -10 μ s (Figure 9c). The former is consistent with a current of

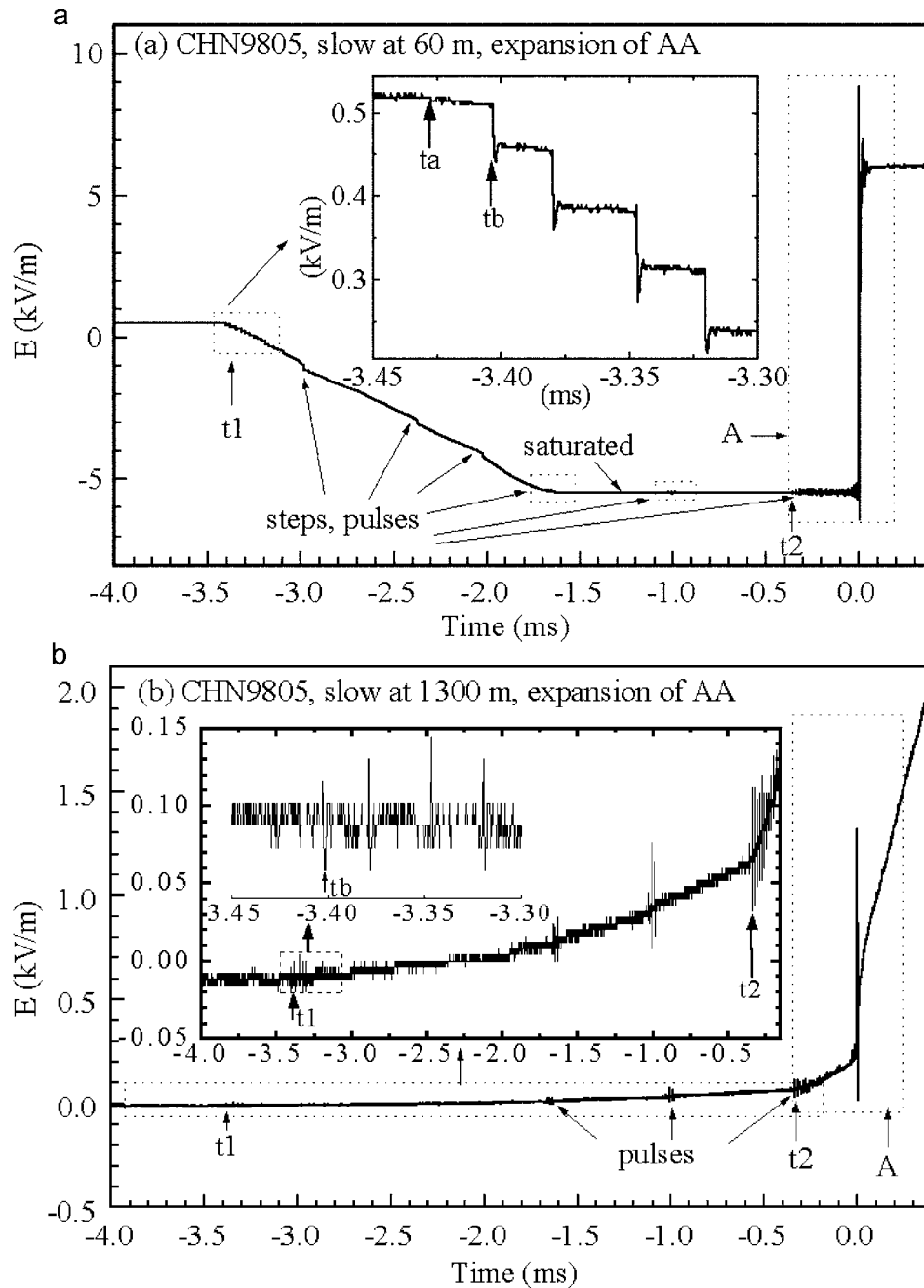


Figure 5. The expansions of the portions “AA” in (a) Figure 3a and (b) Figure 3b. The electric field steps and pulses in the figures are due to the bidirectional leader developments. Time t_1 and t_2 are the onset time of the stable upward positive leader and that of the stable downward negative leader, respectively.

184 A, and the later a current of 359 A. This field slope increase indicates that the upward positive leader accelerates further as the downward negative leader enters its stable propagation regime from t_2 .

3.2. Mini-Return Stroke and Later Discharge Processes

[15] About 345 μ s after the downward negative leader starts its stable propagation, at time -3.6μ s, a light pulse

at the segment of 0–55 m is detected by the ALPS (Figures 4b and 10a). This light pulse is obviously attributed to an upward connecting leader from ground. Connection between the downward negative leader and this upward connecting leader is estimated to be at time t_3 ($t_3 = -1.6 \mu$ s), as the light signals for both segments 0–55 m and 55–111 m begin to increase continuously from that moment (Figures 4b and 10a). The connecting process temporally corresponds to a narrow unipolar field pulse

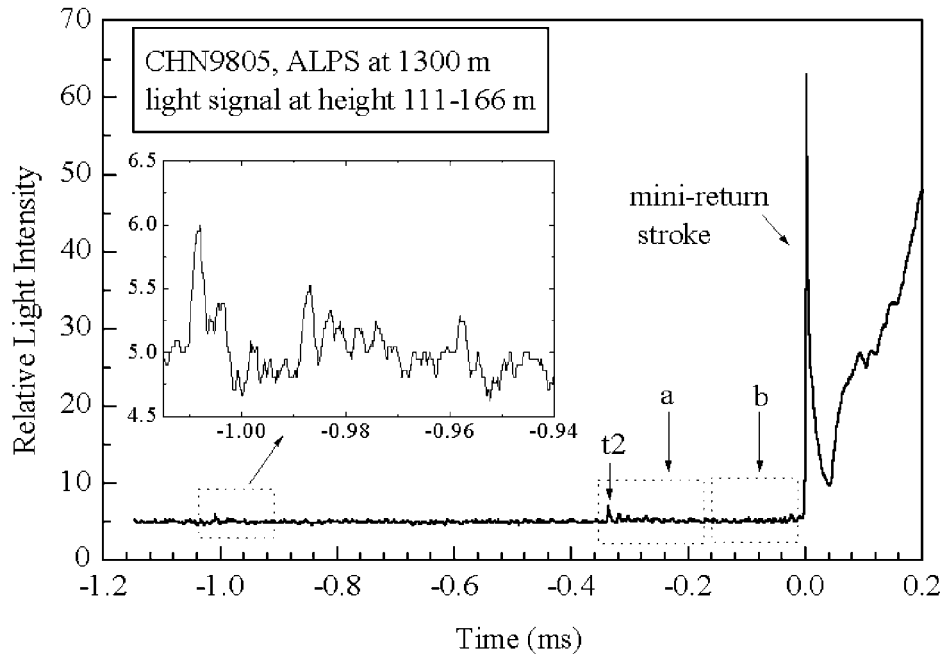


Figure 6. Light signal records of the ALPS for the channel segment 111–166 m of flash CHN9805, showing the light pulses produced by the downward negative stepped leader at the bottom end of the floating wire.

with a half-peak width of only $0.2 \mu\text{s}$ at Site 1 (“P1” in Figure 10b), but to the slow front of a large field pulse at Site 2 (Figure 10c).

[16] The mini-return stroke occurs at time t_4 ($t_4 = 0$), emitting intensive lights from the channel section below the bottom end of the floating wire (Figures 4b and 10a). The peak value of the relative light intensity is about 200 for segments 0–55 m and 55–111 m, but only 70 for segment 111–155 m (the bottom of the wire) and 0 for segments above. The half-peak width of the mini-return stroke light pulse is about $5 \mu\text{s}$ (Figure 4), quite a lot narrower than that of a normal return stroke. The later is usually $20 \mu\text{s}$ or more [e.g., Jordan *et al.*, 1995]. The electric field of the mini-return stroke at Site 1 (Figure 10b) includes a sharp pulse (“P2” in the figure) superimposed on the rising front of a relatively flat pulse (“P3” in the figure). Its electric field at Site 2 (Figure 10c), however, includes only one large sharp pulse similar in shape to the time derivatives of the mini-return stroke light pulse (curve “time derivative for height 0–55m” in Figure 10a). This suggests that the electric field at Site 2 mainly consists of the radiated component from the mini-return stroke channel near the ground, and the field at Site 1 consists of both the radiated component from the mini-return stroke (“P2” in Figure 10b) and the induced and capacitive component from the whole channel (“P3” in Figure 10b). The upward speed of the mini-return stroke, v_1 , as estimated from the onset of the fast transition of the light pulses for various segments, is about $1.8 \times 10^8 \text{ m/s}$.

[17] About $3 \mu\text{s}$ after the mini-return stroke, at t_5 ($t_5 = 3 \mu\text{s}$, Figures 4b and 10a), a bright discharge appears from the top of the wire. This upper bright discharge becomes

invisible to the ALPS after propagating upward about 275 m with a speed, v_2 , of $5.4 \times 10^7 \text{ m/s}$. Meanwhile, gloomy lights along the wire are observed in the later stage of this upper bright discharge for flashes CHN9801, CHN9802 and CHN9804, indicating that the wire explosion probably occurs at this time. The polarity of the charges carried by this upper bright discharge can be derived from its electric fields (Figures 10b and 10c). Since the time 0 for both sites is associated with the electric field peak of the mini-return stroke near the ground, for any electric signal from the bottom of the lightning channel the arrival time at both sites is the same. On the other hand, an electric signal from the upper part of a lightning channel takes more time than that from the bottom of the lightning channel to propagate to an observation site on ground, and this time difference is very significant for close lightning but small for distant lightning. Therefore, for the upper bright discharge starting at t_5 on ALPS, the beginning time of its electric fields at Site 2 should be the same as on ALPS, t_5 , and that at Site 1 be a time lagging t_5 (say t_5'). The time delay of t_5' to t_5 is estimated to be about $1.2 \mu\text{s}$, by simply dividing the triggering height over the speed of light. Both the electric field after t_5' at Site 1 (Figure 10b) and that after t_5 at Site 2 (Figure 10c) are increasing toward positive, indicating that this upper bright discharge carries positive charges.

[18] Just after the upper bright discharge weakens down, at t_6 ($t_6 = 40 \mu\text{s}$), a bidirectional discharge process starts from the bottom end of the wire (the “lower bidirectional discharge” in Figure 4a. Note for flashes CHN9801, CHN9802, and CHN9803, only the upward part is observed). Apparently, the occurrence of this bidirectional discharge is associated with the disintegration of the float-

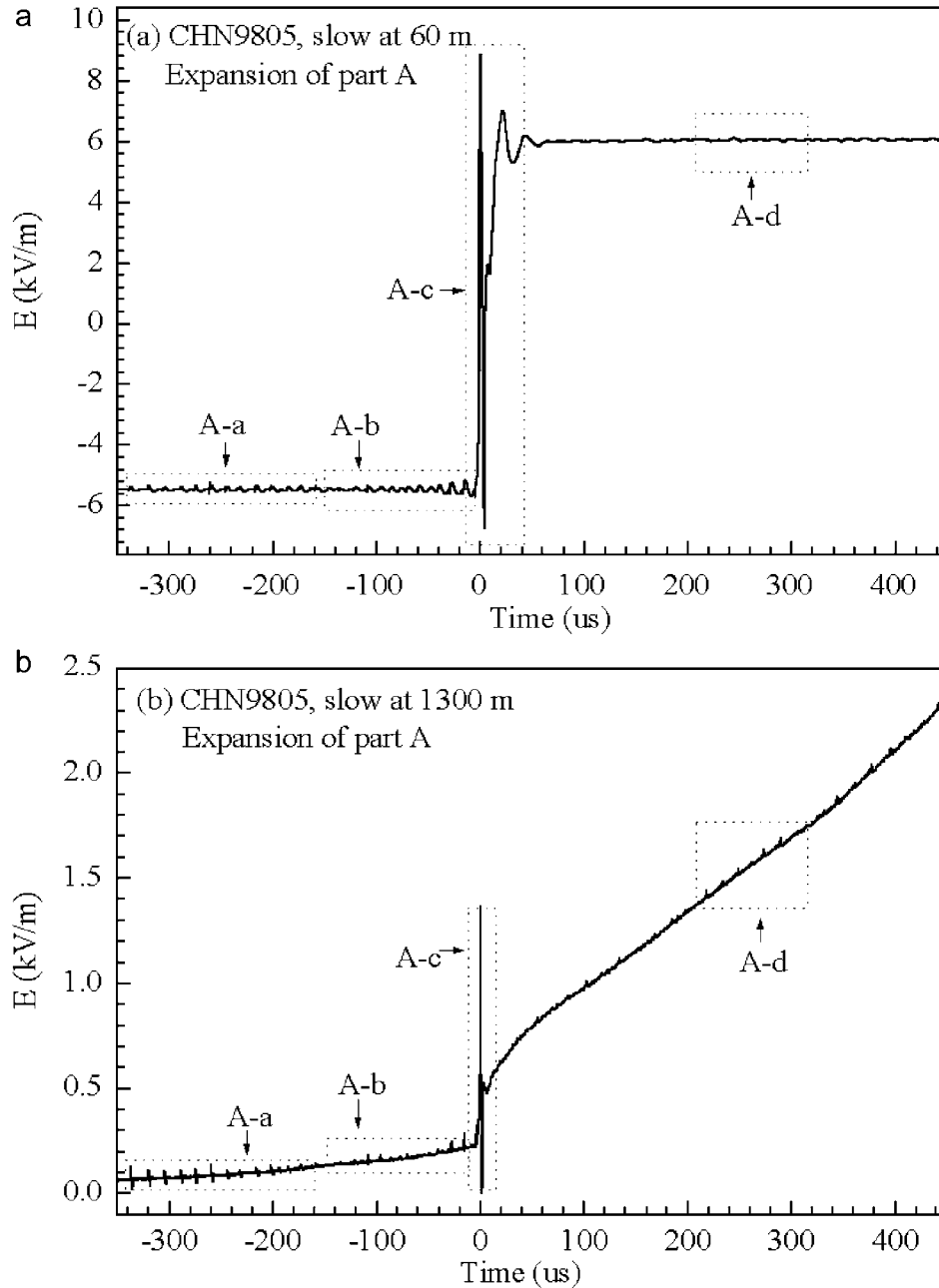


Figure 7. Expansions of the portions “A” in (a) Figure 5a and (b) Figure 5b.

ing wire at the moment. The upward part (the “upward discharge” in Figure 4a) of this bidirectional discharge has a speed v_3 , of 5.5×10^5 m/s, and its downward part (the “downward discharge” in Figure 4a) a speed v_4 , of 2.6×10^5 m/s. Simultaneously with this bidirectional discharge, a negative dart-stepped leader appears from the segment 608–663 m and propagates downward with a speed of about $1.8\text{--}2.7 \times 10^7$ m/s. This dart-stepped leader is observed for flash CHN9805 only. The electric field at Site 2 during this bidirectional discharge consists of a series of unipolar pulses superimposed on a continuously rising slope (“A-d” in Figure 7b). These unipolar pulses have a regular time interval of about $15 \mu\text{s}$, similar to that of the

bidirectional leader before the mini-return stroke. Figure 11 is a comparison of the electric field pulses and the light signals for the upward part of this bidirectional discharge during the time $210 \mu\text{s}$ to $310 \mu\text{s}$. As seen in the figure, corresponding to the electric field surges (Figure 11b) and pulses (Figure 11c), there are no visible light pulses at the upward channel tip (see curves for heights 166–221 m and 221–276 m in Figure 11a), but several light surges in the channel behind (see the curve for height 111–166 m in Figure 11a). As will be discussed in section 4, the electrical field pulses in Figure 11c are due to some positive leader steps ahead of the upward discharge that are optically undetectable for ALPS.

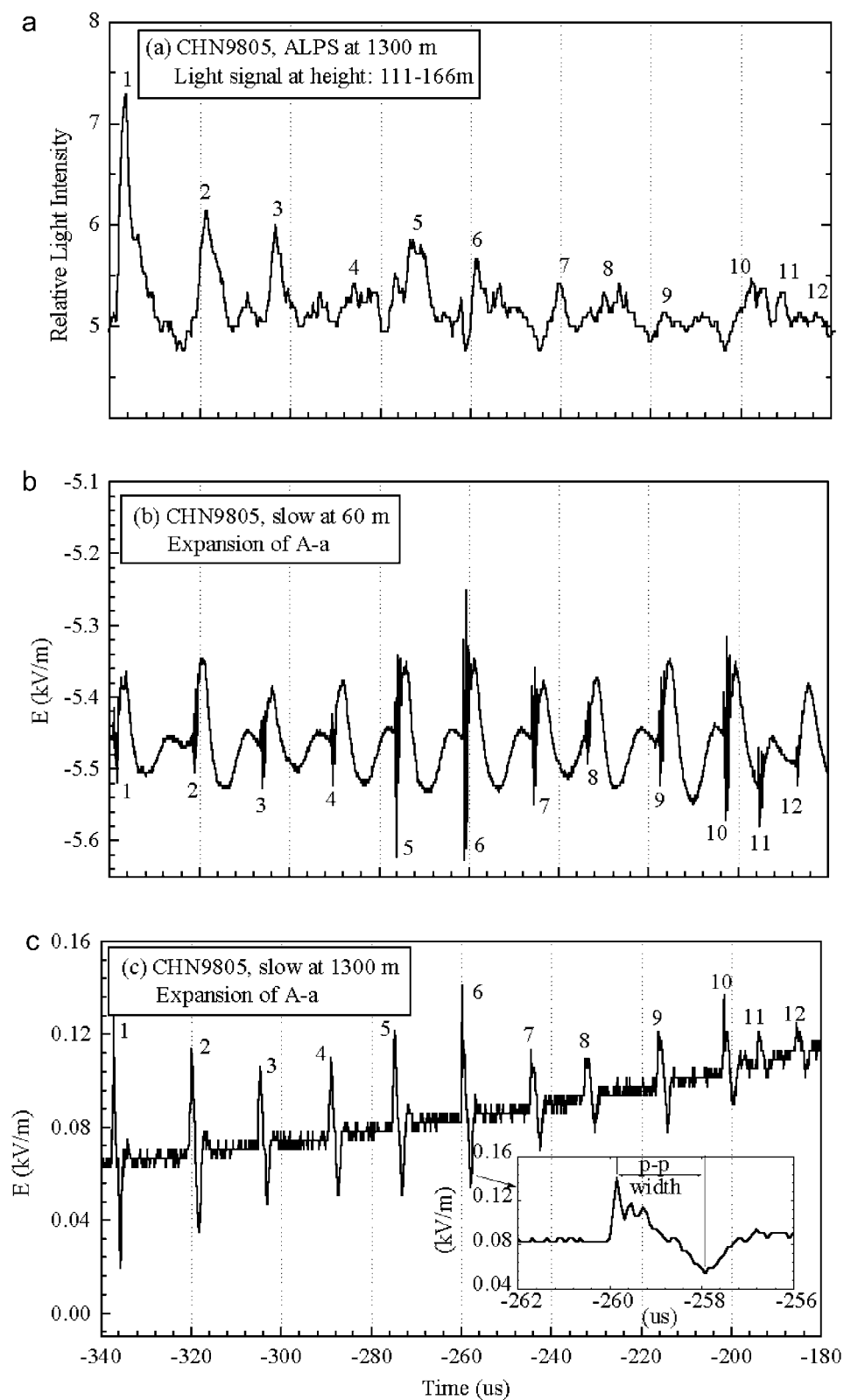


Figure 8. Expansions of (a) the portion “a” in Figure 6, and (b, c) the portions “A-a” in Figures 7a and 7b, respectively.

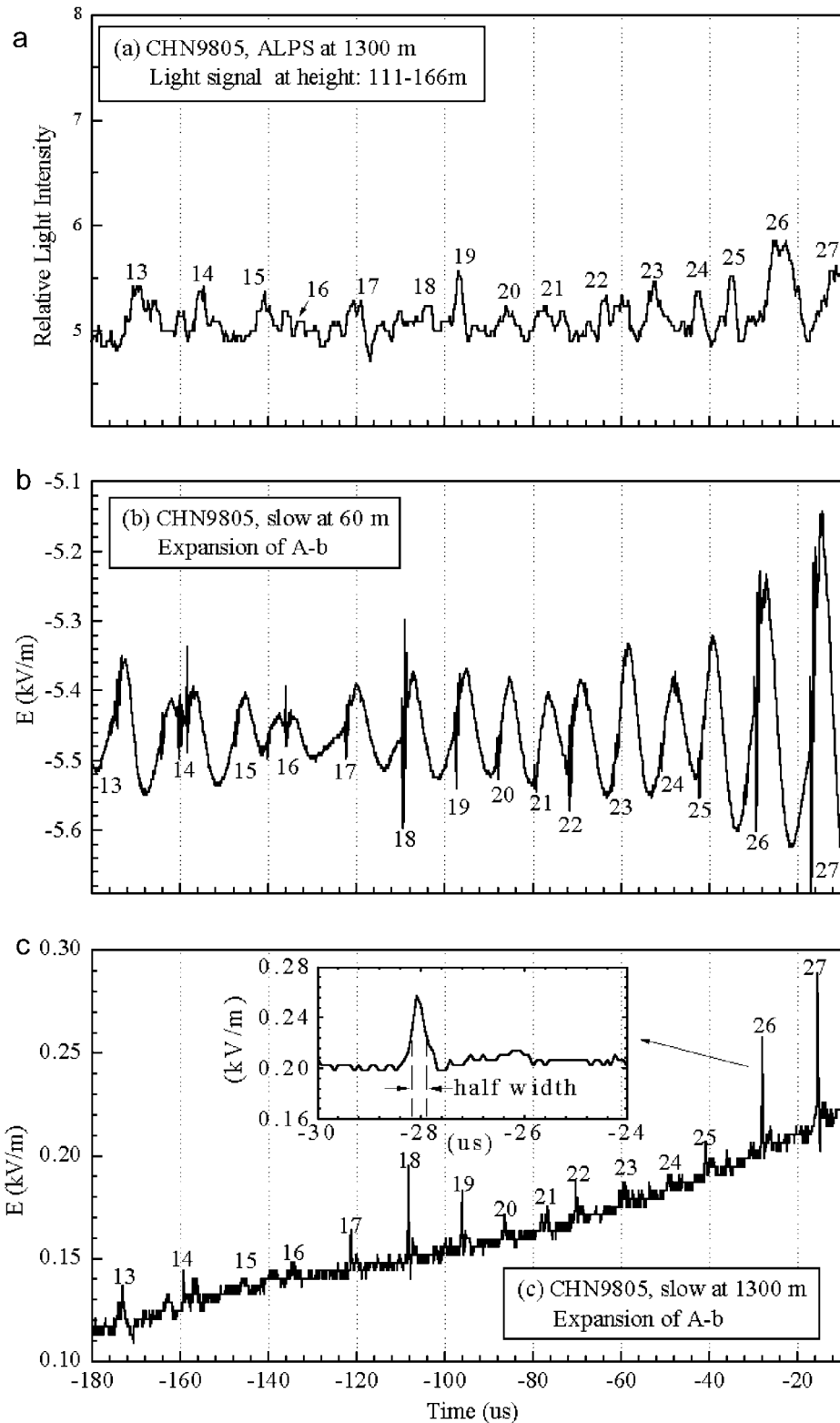


Figure 9. Expansions of (a) the portion “b” in Figure 6, and (b, c) the portions “A-b” in Figures 7a and 7b, respectively.

[19] All of the other four flashes behave similarly, except the specific values of event parameters. These event parameters include the triggering height, the onset time of the bidirectional leader, the speed of the mini-return stroke, the

onset time and speed of the upper bright discharge, as well as the onset time and speed of the lower bidirectional discharge. The event parameters for these 5 flashes are summarized in Table 1, and the main chronological sequence of events

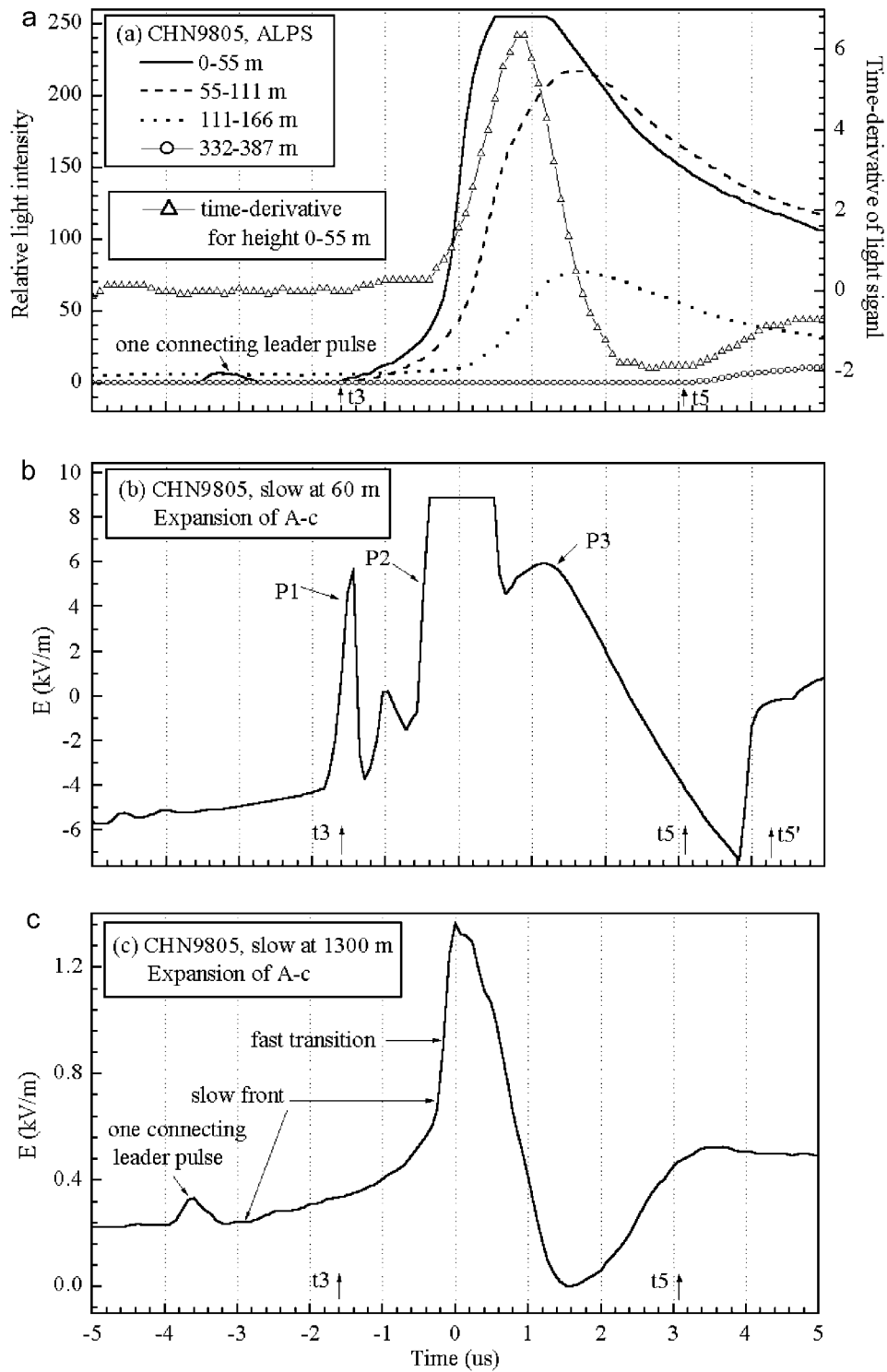


Figure 10. (a) Light waveforms for various heights during the mini-return stroke. The curves 0–55 m, 55–111 m, and 111–166 m are for the mini-return stroke below the bottom of the wire, the curve 332–387 m for the upper bright discharge at the top of the wire, and the time derivatives of the light waveform for the segment 0–55 m. (b, c) Expansions of the portions “A-c” in Figures 7a and 7b, respectively.

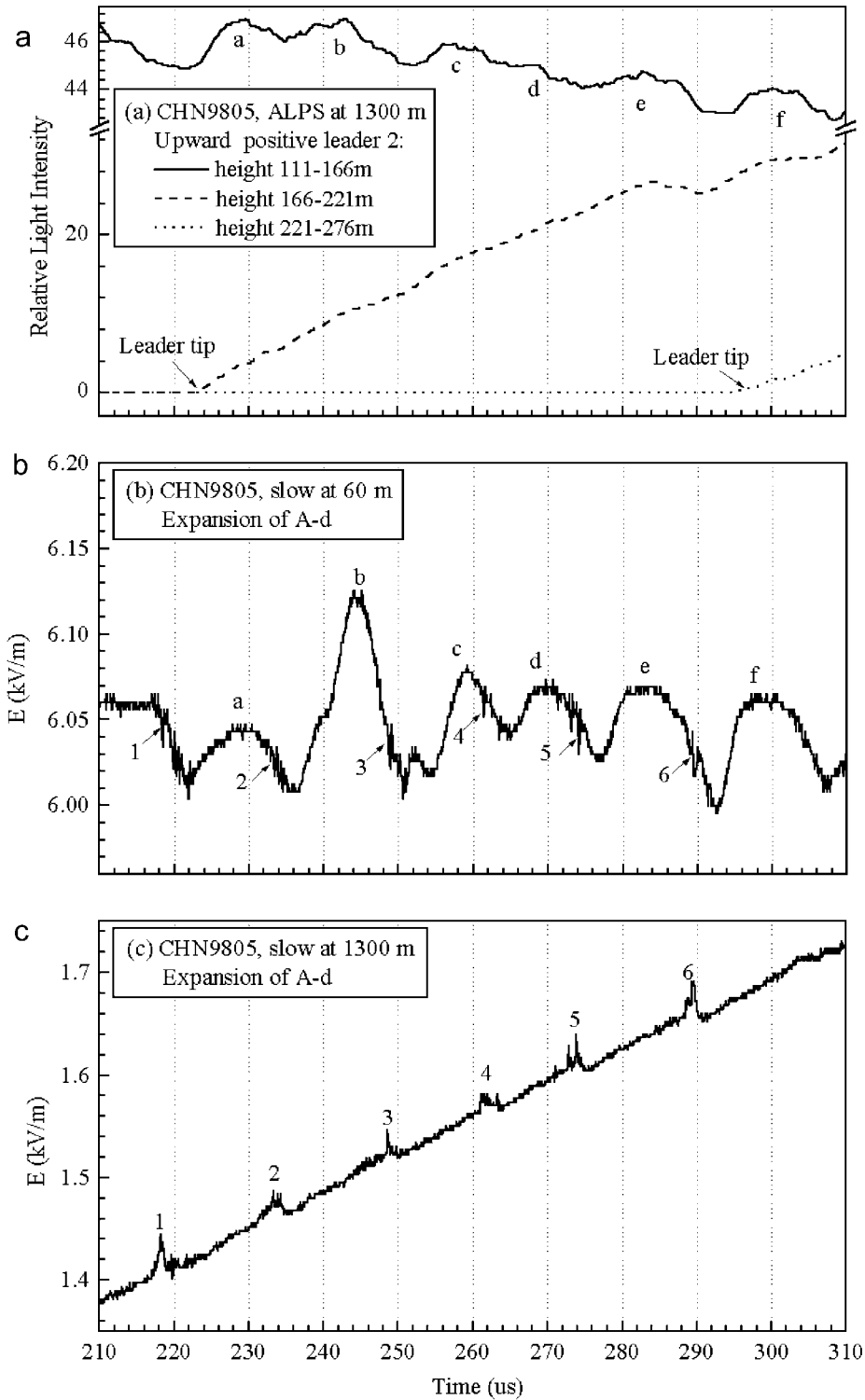


Figure 11. (a) Light waveforms for segments 111–166 m, 166–221 m and 221–276 m, due to the upward part of the lower bidirectional discharge during the time 210 μ s to 310 μ s. (b, c) Expansions of the portions “A-d” in Figures 7a and 7b, respectively.

Table 1. Summary of Statistics on the Five Altitude-Triggered Negative Lightning Flashes^a

Triggering			Bidirectional Leader		Mini-Return Stroke Speed v_1 (10^8 m/s)	Upper Bright Discharge			Lower Bidirectional Discharge		
Flash No.	Time	Height H, m	Onset Time			Onset t_5 , μ s	Length L, m	Speed v_2 (10^7 m/s)	Onset t_6 , μ s	Speed (10^5 m/s)	
			t_1 , ms	t_2 , μ s						v_3 (Up)	v_4 (Down)
9801	16:41:48.97	276	−4.7	−290	1.1	4.1	111	1.5	12	4.0	—
9802	16:45:55.87	553	−8.5	−208	1.4	8.3	276	3.1	10	10.9	—
9803	16:52:22.51	387	−5.5	−350	1.4	3.2	276	4.6	36	3.2	—
9804	16:55:25.13	276	−3.4	−315	1.9	2.7	221	4.4	20	6.1	2.1
9805	17:00:48.66	332	−3.4	−348	1.8	2.9	276	5.4	42	5.5	2.6

^aTriggering heights are determined from the observations of ALPS. Time 0 is associated with the peak of the electric field pulse due to the mini-return stroke.

involved in an altitude-triggered lightning flash as inferred from our observations is schematized in Figure 12.

4. Discussion

4.1. Characteristics of the Bidirectional Leader Before Mini-Return Stroke

[20] For all five cases, it was found that there are always some isolated negative electric field steps prior to the actual onset of the bidirectional leader by several tens of milliseconds at Site 1. The time interval between the isolated field steps is about 5 ms in mean. For the classical triggered lightning, *Lalande et al.* [1998] found that there are some isolated current pulses separated by an average duration of 5 ms in the first phase of the discharge, which they thought to be attributable to a series of aborted positive leader inceptions from the top of the grounded wire. Similar to the classical triggered lightning, the isolated negative electric field steps observed for the altitude-triggered lightning here might be associated with the aborted positive leader inceptions from the top of the floating wire. As in the classical triggered lightning, the top of the floating wire in altitude-triggered lightning is ascending in a quasi-stationary field produced by thunderclouds. When the electric field intensity at the ascending rocket tip increases to the inception threshold for a positive leader, which is lower than that for a negative leader [*Les Renardieres Group*, 1972, 1981], a positive leader may start there first. This positive leader will cease after propagating upwards for a few meters due to the shielding effects of local corona charges around the leader tip. The next attempt of the positive leader inception could not occur until the motions of the ion drifting and rocket ascending restore the local field. The time interval between the attempts of the positive leader inception is associated with the local electric field restoration circle, depending on the size of the corona region, the drift velocity of the ions, and the ascending speed of the wire top. Each attempt of the positive leader produces a current pulse that injects a negative charge into the floating wire. Under a quasi-stationary field of the thunderclouds, this negative charge will finally concentrate in the lower part of the floating wire. It is this negative charge in the floating wire that produces negative field step changes at the closer Site 1. If the magnitude of the negative charge involved in an attempt of the positive leader is enough to enhance the local field at the bottom of the floating wire to the threshold for a negative leader inception, a negative leader attempt may occur also. The charges involved in the isolated electric field step changes are estimated to be about ± 20 to ± 40 μ C.

These values are two orders smaller than the individual step charge estimated for lightning leaders by *Krider et al.* [1977] and *Rakov et al.* [1998], but consistent with those observed for positive laboratory leaders by the *Les Renardieres Group* [1972] and for negative laboratory leaders by *Bondiou-Clergerie et al.* [1996]. The average current that must flow in the wire to deposit this amount of charge at the two ends of the wire is estimated to be about 20 A to 27 A, one order smaller than that estimated for a natural lightning leader. The electric field radiated by such a small current may be too weak to be detected at Site 2. Therefore, it is reasonable to think that the isolated negative electric field steps are attributed to a series of attempted inception of an upward positive leader from the top of the floating wire.

[21] For the altitude-triggered lightning flashes studied by *Laroche et al.* [1991] and by *Lalande et al.* [1998], no isolated field steps before the actual onset of the bidirectional leader were observed. This is probably because the distances from the bottom of the floating wire to the sensors at ground level in their experiments is too long, so that the electric field change due to a small negative charge at the bottom of the wire could not be detected.

[22] The actual onset of the upward positive leader should be around time t_1 ($t_1 = -3.4$ ms), as indicated by its electric field at Site 2 which includes a series of bipolar pulses superimposed on the beginning of a continuously rising slope starting from t_1 (Figure 5b). Its electric field at Site 1 begins to decrease from t_1 first step-wisely and then continuously (Figure 5a). As discussed above, the development of the positive leader leaves positive charges in its channel and the upper part of the wire, and injects negative charges into the lower part of the wire. Since the electric field at Site 1 is mainly subjected to the charges in the lower part of the wire and that at Site 2 to the charges in the upper part of the wire, the upward positive leader produces negative field changes at the Site 1 and positive field changes at the Site 2. On the other hand, a negative electric field step at Site 1 may be produced by a downward negative leader step from the bottom of the wire also. The first field step around t_1 (Figure 5a) is consistent with a charge of -50 μ C at the bottom of the wire and a transit current of about 100 A. Such a small charge could not be associated with a mature negative leader step, but may be associated with an aborted one. The first step of the downward negative leader detected by ALPS is at the time -1.0 ms (Figure 6), which lags the first step of the upward positive leader by more than 2 ms. The stable propagation of the downward negative stepped leader starts at time t_2 ($t_2 = -348$ μ s), about 3 ms after the onset of the upward

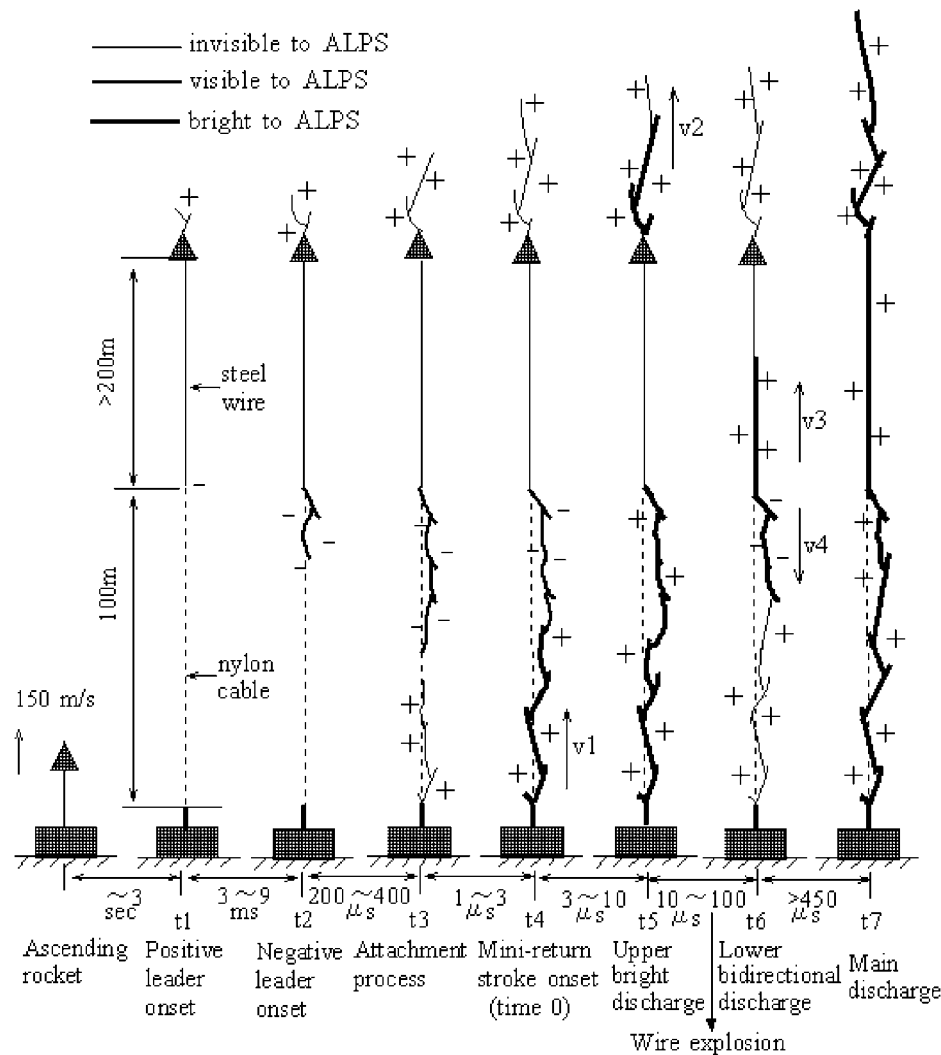


Figure 12. Schemata of the main chronological sequence of events involved in an altitude-triggered negative lightning flash as inferred from the electric fields and lights measurements made for five triggered lightning flashes on August 22, 1998, China.

positive leader. These are consistent with the results of Laroche *et al.* [1991] and Lalande *et al.* [1998] for altitude-triggered negative lightning. In classical triggered lightning, field step/pulse changes were observed to accompany the inceptions of both the negative and positive leaders from the top of the triggering wire (e.g., Laroche *et al.* [1988] and Lalande *et al.* [1998] for upward positive leaders; Chen *et al.* [1999b] and Horii *et al.* [1996] for upward negative leaders). For an altitude-triggered positive lightning flash with the bottom end of the floating wire being 130 m high and the grounded intercepting wire being 50 m long [Chen *et al.*, 1999b], the inception of the bidirectional leader was also accompanied by several step/pulse electric field changes. However, the onset of the upward negative leader of the bidirectional leader system in the altitude-triggered positive flash was prior to that of the downward positive leader by only few microseconds.

[23] The electric field pulses at Site 2 in the earlier stage of the bidirectional leader development have a well-defined bipolar shape (p-p width ranges from 1 to 2 μs , Figure 8c),

while those in the latter stage have a unipolar shape (about 0.4 μs in half-peak width, Figure 9c). Similar results were observed for both the “classical” and “altitude” triggered positive lightning flashes [Chen *et al.*, 1999b]. For the downward negative stepped leader in a cloud-to-ground discharge, the electric field pulses in the earlier stage of the leader developments, typically 10–20 ms before the return stroke, are large bipolar ones [Weidman and Krider, 1979], while those in the latter stage usually a few hundred microseconds before the return stroke are narrow unipolar ones [Krider *et al.*, 1977; Beasley *et al.*, 1982, 1983].

[24] To explain why there is such a difference in the shapes of the electric pulses radiated by a stepped leader during its various development stages, let us have a following discussion first.

[25] For a current pulse $i(t)$ propagating from height z_1 up to z_2 ($z_2 > z_1$) vertically at a constant speed v on an exponential loss transmission line [Nucci *et al.*, 1988], the vertical electric field at a point on the ground with a relative remote distance D from the channel base due to the current

in a channel element dz is approximately given by [see *Uman, 1987*],

$$dE(D, t) = -\frac{1}{2\pi\epsilon c^2 D} \frac{\partial i(z, t - D/c)}{\partial t} dz \quad (1)$$

$$i(z, t) = e^{-(z-z_1)/L} i(z_1, t - (z - z_1)/v), \quad (2)$$

where c is the light speed, ϵ the dielectric constant of air, L a distance constant representing the current attenuation rate, and t the time. The time-derivative of equation (2) is as follows:

$$\frac{\partial i(z, t)}{\partial t} = -v \left[\frac{\partial i(z, t)}{\partial z} + \frac{1}{L} i(z, t) \right]. \quad (3)$$

Bringing equation (3) into equation (1) with the time referred to the start of the current, equation (1) becomes

$$dE(D, t + D/c) = \frac{v}{2\pi\epsilon c^2 D} \left[\frac{\partial i(z, t)}{\partial z} + \frac{i(z, t)}{L} \right] dz. \quad (4)$$

Integrating equation (4) over z_1 to z_2 , we have the following equation:

$$E(D, t + D/c) = \frac{v}{2\pi\epsilon c^2 D} \left[i(z, t) \Big|_{z_1}^{z_2} + \frac{1}{L} \int_{z_1}^{z_2} i(z, t) dz \right]. \quad (5)$$

As shown in equation (5), for a current pulse $i(z, t)$, regardless of whether it has a unipolar or a bipolar shape, the right first term of equation (5) tends to be a bipolar pulse. The extent of this bipolar pulse depends on the time delay and amplitude difference of the current at the two heights z_1 and z_2 . The right second term of equation (5) is usually similar to its causative current waveform. For a current pulse propagating along its path without attenuation (i.e., $L = \infty$) or with little attenuation (i.e., $L \gg z_2 - z_1$), the total electrical field will be dominated by the right first term of equation (5), and exhibit a well-defined bipolar shape. When the current attenuates seriously along its propagating path (i.e., $L \ll z_2 - z_1$), both terms on the right of equation (5) have similar shapes to its causative current waveform. In addition, equation (5) shows that the longer the path that the current pulse propagates, the wider the electric field pulse produced by the current pulse.

[26] Let us apply this theory to our altitude-triggered lightning. In the earlier stage of the bidirectional leader development, the channel of the upward positive leader is short and its tip is close to the top of the floating wire. A current pulse due to an individual step of the upward positive leader injects into the wire with little attenuation. This current pulse continues to propagate along the wire down to the wire bottom without losses to trigger a bright negative leader step there (Figure 8a), and produces a bipolar electric field pulse at Site 2 (Figure 8c). As the upward positive leader channel extends, a current pulse due to an individual step at the leader tip suffers severe attenuation when propagating back down in its long leader channel. Consequently, the current pulse when coming down to the wire is already blunt and very weak. This

blunt and weak current pulse propagates down to the bottom of the wire to trigger a less bright negative leader step there (Figure 9a), and produces a unipolar electric field pulse at Site 2 (Figure 9c). For the natural downward negative stepped leader, the bipolar field pulses in the earlier stage of the leader developments may come from some short breakdown discharges inside the thundercloud where the discharge current suffers little attenuation when traveling in its discharge channel. The unipolar electric field pulse in the later stage of the leader development may be attributed to the severe attenuation of the current pulse of a leader step within the leader channel. Actually, observations on two negative downward stepped leaders by *Chen et al. [1999a]* indicated that a sharp step current pulse declined into a flat current surge after propagating only several tens of meters from the leader tip back.

4.2. Characteristics of the Mini-Return Stroke and the Later Discharges

[27] The properties of the mini-return stroke can be summarized into the following two points. (1) It emits intensive light only below the bottom end of the floating wire, with the half-peak width of the light pulse being about 5 μ s. This is because the minireturn stroke current enters and follows the metallic wire, which is still alive. (2) The electric field at Site 1 includes two unipolar pulses, with the half-peak width of the first pulse being just 0.2 μ s (the “P1” and “P2” in Figure 10b), while that at Site 2 includes only one bipolar pulse with its half-peak width being much narrower than that of a normal return stroke (Figure 10c). Temporally, the field pulses P1 and P2 in Figure 10b correspond to the slow front and the fast transit edge of the mini-return stroke light pulse in Figure 10a, respectively. Similar properties on close electric fields and base currents were observed for a positive altitude-triggered lightning flash by *Chen et al. [1999b]*, and for a negative altitude-triggered lightning flash by *Rakov et al. [1998]*, except that the first pulse in their studies (several microseconds in half-peak width) is wider than that in this study. A probable explanation for this is that the first pulse P1 is associated with the upward connecting leader, and the second pulse P2 with the main minireturn stroke. As discussed in section 4.1, for the cases of *Chen et al. [1999b]* and *Rakov et al. [1998]*, the current pulse of the connecting leader propagating to Earth through a 50-m-long intercepting wire, produced a relatively wider electric field pulse at close distances. While, for this study, no intercepting wire was employed, and the path of the connecting leader current pulse was only several meters long, producing a relatively narrower electric field pulse P1 at the close Site 1. Since the pulse P1 (the half-peak width is 0.2 μ s) contains many high-frequency components and its source is near the ground, it suffers severe attenuation when propagating on the ground surface. As a result, it could not be detectable even at Site 2. The difference in the waveforms of the light and the electric field between a mini-return stroke and a normal return stroke, as explained by *Rakov et al. [1998]*, is apparently due to the relatively short length of the channel available for the upward propagating of the mini-return stroke wave.

[28] The upper bright discharge following the mini-return stroke is undoubtedly transformed from the mini-return stroke wave (Figure 4b). Propagating in the channel built

by the previous positive leader, this upper bright discharge is brighter and faster than the previous positive leader. Its cessation is apparently due to the wire explosion that interrupts the charge transfer between ground and the upper bright discharge channel.

[29] The lower bidirectional discharge following the upper bright discharge is probably due to the reflection of the mini-return stroke current at the bottom end of the exploded wire (Figure 4a). With the explosion of the floating wire, the connection between the upper bright discharge and ground is interrupted suddenly. The upward current wave in the low impedance mini-return stroke channel has to terminate its journey at the bottom end of the wire, with part of it transforming into an upward positive discharge along the wire residue and part of it being reflected downward to form a downward negative discharge along the “dead” mini-return stroke channel. As the path that this upward positive discharge follows is not ionized perfectly, there are some positive leader step processes occurring ahead of the channel of this upward positive discharge, producing a series of unipolar electric field pulses superimposing on a rising slope (Figure 7b).

5. Summary

[30] Five negative lightning flashes triggered using the “altitude” technique have been studied. The main chronological sequence of events involved in these flashes, as inferred from the simultaneous measurements of two-station electric fields and highly space- and time- resolved light signals, is schematized in Figure 12.

[31] As shown in Figure 12, when the rocket ascends to 300-m to 500-m high above ground, after two or three inception attempts an upward positive leader is initiated from the top of the floating wire at the time t_1 first. This upward positive leader propagates first in a discontinuous pattern made of successive re-strikes of a similar time period and then in a continuous pattern. Several milliseconds later, a downward negative stepped leader is initiated from the bottom end of the wire, forming a bidirectional leader system. This downward negative stepped leader stops and starts several times as the upward positive one propagates forward continuously, and finally enters its stable propagation regime at t_2 . When the downward negative stepped leader is close to ground, a so-called mini-return stroke occurs. This mini-return stroke emits intense light below the bottom of the wire and becomes invisible when entering the wire. Several microseconds later, this mini-return stroke appears again from the top of the wire as a bright positive discharge with an upward speed of $1.5\text{--}5.4 \times 10^7$ m/s. This upper bright positive discharge becomes optically undetectable after extending forward several hundred meters due to the wire explosion at the moment. Just after the cessation of this upper bright positive discharge, a bright bidirectional discharge process starts from the bottom end of the wire. The occurrence of this lower bidirectional discharge may be due to the reflection of the upward mini-return stroke current wave at the bottom end of the exploded wire.

[32] **Acknowledgments.** The authors thank cordially the members of Gifu University of Japan, Lanzhou Institute of Plateau Atmospheric Physics of the Chinese Academy of Sciences, and Guangdong Power Test and Research Institute for their help in the field experiments. The authors would also like to thank the reviewers for their valuable suggestions on revising the paper. The work leading to this paper was supported in part by a grant from the Research Committee of The Hong Kong Polytechnic University.

References

- Beasley, W. H., M. A. Uman, and P. L. Rustan, Electric field preceding cloud-to-ground lightning flashes, *J. Geophys. Res.*, **87**, 4883–4902, 1982.
 - Beasley, W. H., M. A. Uman, D. M. Jordan, and C. Ganesh, Simultaneous pulses in light and electric field from stepped leaders near ground level, *J. Geophys. Res.*, **88**, 8617–8619, 1983.
 - Bondiou-Clergerie, A., G. L. Bacchiega, A. Castellani, P. Lalande, P. Laroche, and I. Gallimberti, Experimental and theoretical study of the bi-leader process: I. Experimental investigation, paper presented at 10th International Conference on Atmospheric Electricity, Int. Comm. of Atmos. Electr., Osaka, Japan, June 10–14, 1996.
 - Chen, M., N. Takagi, T. Watanabe, D. Wang, Z.-I. Kawasaki, and X. Liu, Spatial and temporal properties of optical radiation produced by stepped leaders, *J. Geophys. Res.*, **104**, 27,573–27,584, 1999a.
 - Chen, M., et al., Leader properties and attachment process in positive triggered lightning flashes, *J. Atmos. Electr.*, **19**, 45–59, 1999b.
 - Horii, K., et al., Triggered lightning experiments in 1994–1995 for winter thunderstorms, paper presented at 10th International Conference on Atmospheric Electricity, Int. Comm. of Atmos. Electr., Osaka, Japan, June 10–14, 1996.
 - Jordan, D. M., V. P. Idone, R. E. Orville, V. A. Rakov, and M. A. Uman, Luminosity characteristics of lightning M components, *J. Geophys. Res.*, **100**, 25,695–25,700, 1995.
 - Krider, E. P., C. D. Weidman, and R. C. Noggle, The electric fields produced by lightning stepped leaders, *J. Geophys. Res.*, **82**, 951–960, 1977.
 - Lalande, P., A. Bondiou-Clergerie, P. Laroche, A. Eybert-Berard, J.-P. Berlandis, B. Bador, A. Bonamy, M. A. Uman, and V. A. Rakov, Leader properties determined with triggered lightning techniques, *J. Geophys. Res.*, **103**, 14,109–14,115, 1998.
 - Laroche, P., V. Idone, L. Barret, Observations of bidirectional leader development in triggered lightning flash, paper presented at the International Conference on Lightning and Static Electricity, NASA, Cocoa Beach, Fla., April 16–19, 1991.
 - Les Renardières Group, Research on long air gap discharges, *Electra*, **23**, 53–157, 1972.
 - Les Renardières Group, Negative discharges in long air gaps, *Electra*, **74**, 67–216, 1981.
 - Nucci, C. A., C. Mazzetti, F. Rachidi, M. Ianoz, On lightning return stroke models for LEMP calculations, paper presented at 19th International Conference on Lightning Protection, Conv. of Natl. Soc. of Electr. Eng. of Eur., Graz, Austria, 25–29 April, 1988.
 - Rakov, V. A., et al., New insights into lightning processes gained from triggered-lightning experiments in Florida and Alabama, *J. Geophys. Res.*, **103**, 14,117–14,130, 1998.
 - Uman, M. A., The lightning discharge, 329 pp., Academic, San Diego, Calif., 1987.
 - Wang, D., V. A. Rakov, M. A. Uman, N. Takagi, T. Watanabe, D. E. Crawford, K. J. Rambo, G. H. Schnetzer, R. J. Fisher, and Z.-I. Kawasaki, Attachment process in rocket-triggered lightning strokes, *J. Geophys. Res.*, **104**, 2143–2150, 1999.
 - Weidman, C. D., and E. P. Krider, The radiation field waveforms produced by intracloud lightning discharge processes, *J. Geophys. Res.*, **84**, 3157–3164, 1979.
- M. Chen and Y. Du, Department of Building Services Engineering, Hong Kong Polytechnic University, Hung Hom, Kowloon, Hong Kong. (bemchen@polyu.edu.hk; beydu@polyn.edu.hk)
- X. Liu, Cold and Arid Regions and Environmental Engineering Institute, Chinese Academy of Sciences, 2066 Donggang West Road, Lanzhou, Gansu, China. (xslu@ns.lzb.ac.cn)
- N. Takagi, D. Wang, and T. Watanabe, Department of Electrical and Electronic Engineering, Gifu University, 1-3 Yanagido, Gifu City, Japan. (takagi-n@cc.gifu-u.ac.jp; wang@cc.gifu-u.ac.jp; watanabe@cc.gifu-u.ac.jp)